SUPPLEMENTARY MATERIALS

MATERIALS AND METHODS

Transgenic Mice

Transgenic mice with c-Myc overexpression were generated from a modified pCAGEN vector backbone[1] containing PmeI sites flanking the CAG promoter[2] and rabbit beta-1 globin gene polyadenylation sites to allow for exclusive excision of the transgenic sequence. A Lox-STOP-Lox element[3], N-terminal HA-epitope tagged c-Myc (human), EMCV IRES[4], and palmitoylated-eGFP[5] were cloned and sequences inserted between the CAG promoter and the downstream beta-1 globin gene untranslated sequences containing polyadenylation sites to generate a Cre-activateable bicistronic mRNA capable of simultaneous expression of HA-tagged Myc and palmitoylated GFP in a wide array of cells and tissues (see fig. S1A). Myc^{Tg} mice were created via pronuclear injection of the purified PmeI digested fragment containing the transgene sequence into C57Bl/6 zygotes by the Gladstone Institutes transgenic core facility. Myc^{Tg} mice were maintained on a C57BL/6J background and crossed with Pb-cre4;$Pten^{fl/fl}$ mice (described elsewhere)[6] maintained on a C57BL/6J background for *in vivo* experiments. Mating crosses were completed with Pb-Cre4 present only through the paternal line to prevent leaky or loss of Cre expression during embryogenesis or within oocytes. PERK floxed mutant mice possess loxP sites flanking exon 3-5 of the Eif2ak3 gene were obtained from The Jackson Laboratory (stock 023066). All mice were maintained under specific pathogen-free conditions. Experiments were performed in compliance with guidelines approved by the Institutional Animal Care and Use Committee of UCSF.

In vivo phenotypical penetrance analysis

GEMMs were euthanized at 6 and 10 weeks for prostate microdissection. Tumor progression was analyzed from serial sectioned, formalin-fixed paraffin embedded tissue stained by Haematoxylin and Eosin (H&E). Prostate lobes were examined for abnormalities based on cell size and shape scored on progression from low to high-grade prostatic intraepithelial neoplasia (PIN) confirmed by urologist at UCSF. Neoplasia grade is scored by the apparent progression of abnormal cells with enlarged and darkened nuclei and nucleoli, components of the nuclei that aid in ribosome biogenesis to promote protein production. If abnormal cells have filled the inner duct, showing high malignant proliferation rupturing gland structure, the gland is scored as adenocarcinoma.

Dry weight measurements

All GEMM prostates were dissected at the indicated times, formalin fixed overnight, and dehydrated to 70% Ethanol. For measurements, prostate lobes were microdissected and separated to allow full drying prior to weighing. Weights per genotype at a given age were averaged for three or more mice.

In vivo tumor measurements

Ultrasound analysis was completed using either the Vevo 770 or 2100 ultrasound imaging system taking videos of individual prostate tumors per mouse. The widest image was captured from video and measurements calculated per tumor for each mouse. The largest

tumor detected per mouse was used to represent individual mouse tumor size and then averaged for each genotype at indicated age for comparison.

Survival study

Cohorts of mice were aged till they showed signs of distress monitored by body conditioning score ≤ 2 (bones protruding at lower spine), rapid weight loss or gain of 10% body weight, or by measuring tumor diameter not to exceed 2 cm viewable by ultrasound. Once internal tumors were detected, viewable first by abdominal swelling and then potentially by ultrasound, mouse health and activity were monitored daily. At terminal-stage, mice are fully dissected for evaluating potential metastatic lesions, and prostatic tissues microdissected and processed for pathological analysis.

Organoid culturing

Mice of same age were euthanized, and prostate tissue was microdissected. Three independent sets of organoids were used to confirm analysis for biological replicates per genotype (age of mice per individual sets were 8, 10, and 12 weeks old). Upon full removal of adipose, seminal vesicles, urethra, and bladder, each lobe was detached in PBS to further remove any non-prostatic tissues. Lobes were pulled, minced, and digested in 2 mg/mL Collagenase II (dissolved in ADMEM/F12) with Y-27632 (1 μM) for 1-2 hr at 37°C gently rotating. Minced prostatic fragments were washed in 3 mL of TrypLE and digested for approximately 15 min at 37 ºC with vortexing every 5 min. Once washed in ADMEM/F12, remaining cells were briefly syringed through 18 and 20-gauge needles followed by straining to single cell. Approximately 20,000 cells were seeded within 50 uL of Matrigel to 24-well warmed plates to solidify and then 500 μL of murine prostate medium added [ADMEM/F12 medium supplemented with B27 (life technologies), 10 mM Hepes, Glutamax, n-acetyl cysteine 1.25 mM, penicillin streptomycin (P/S), mEGF 50 ng/mL, NOGGIN 100 ng/mL, R-SPONDIN 500 ng/mL, A83-01 200 nM, DHT 1nM, and Y-27632 10μM][7]. Organoids were frozen down after successful propagation with validation through genotyping DNA and evaluating relevant phenotypes by western. For culturing, organoids were split 1:4 or less weekly by TrypLE for 10 min, then seeded in similar manner by counting single cells per experiment.

Western Blot Analysis

Western blot analysis was performed using standard procedures with commercial antibodies for GFP (Santa Cruz); Cell signaling antibodies: P-PERK, PERK, P-eIF2α, eIF2α, PTEN, P-AKT Ser^{473}, C-MYC, Cleaved Caspase-3 (Asp175); ATF4 (ProteinTech); AR (Abcam); and β-actin (Sigma). Where mentioned, protein levels were quantified using ImageJ software to analyze optical density of western blots normalized to loading control.

Analysis of Global Protein Synthesis *ex vivo*

Organoid cultures were pulsed with 50 μCi of 35S labeled methionine/cysteine added to the media and incubated for 1 hr. For ISRIB experiments, cells were treated for 5 hr with the addition of DMSO or ISRIB prior to additional 1 hr pulse with 35S labeled methionine/cysteine. Three independent biological sets of organoids were tested at least once and used for analysis. Cell lysates were prepared using standard procedures and equal amounts of total protein were separated out on a 10% SDS polyacrylamide gel and

transferred to PVDF membrane. Membranes were exposed to autoradiography film for extended period. 35S methionine/cysteine incorporation was quantified using ImageJ software to analyze optical density and normalized to β-actin on same membrane.

Immunofluorescence and immunohistochemistry microscopy

Tissue from GEM and PDX models were dissected directly to formalin for overnight fixation rotating at 4 °C followed by dehydration, and then paraffin embedding by Core Facility. Tissue was sectioned and slides de-waxed and rehydrated in an alcohol series followed by antigen retrieval with citrate solution. Sections were blocked according to secondary in 5% serum and 1% BSA with or without 0.2% Triton X-100 in TBS for 60 min at 25°C. Immunostaining was performed with labeled primary antibodies overnight at 4°C. Expression was detected with corresponding fluorochrome-conjugated secondary antibodies (Invitrogen) and nuclei were stained with a DAPI mount (Vector Laboratories). For immunohistochemistry, expression was detected with corresponding avidin DH-biotinylated horseradish peroxidase complex for 30 minutes (Vectastain ABC Elite Kit, Vector Laboratories) and subsequently washed and incubated with biotin-conjugated secondary antibodies for 30 minutes. After applying enzyme-conjugated secondary, samples were developed with the diaminobenzidine substrate Kit (Vector Laboratories) and counterstained with hematoxylin to show nuclei.

Images were taken with a Zeiss AxioImager M1 Upright Microscope. Quantifications were performed as the fluorescence per area or mean fluorescence intensity per cell as labeled. For GEMMs, all microscopy focused on anterior prostate. The expression of P-IRE1, P-PERK, or P-eIF2α was quantified relative to DAPI using ImageJ software and at least four images taken at 20x were then averaged per mouse. For ATF6 and Myc antibody staining, nuclear expression was counted and percent determined to total cell count viewed by Dapi for at least four images at 40x magnification per mouse. Fold change plotted is relative to wildtype expression. For PDX samples, the expression of P-AKT, PTEN, c-MYC, CK8, or P-eIF2α was quantified using mean fluorescence intensity of three random cancer areas normalized to adjacent stromal benign area. Ki67 staining were quantified using manual counting.

The following antibodies were used: chicken polyclonal anti-CK8 (Cat#ab107115; Abcam; [1:200]), chicken polyclonal anti-CK5 (Cat#905901; BioLegend; [1:200]), chicken polyclonal GFP (Cat#GFP-1020 ; Aves; [1:200]), P-His3 Ser10 (Cat#06-570; Millipore; [1:200]), rabbit monoclonal anti-c-Myc (Cat#ab32072; Abcam; [1:100]), rabbit polyclonal anti-p-IRE1a (Cat#100-2323; Novus; [1:150]), rabbit polyclonal anti-p-PERK (Cat#3179; Cell Signaling; [1:100]), rabbit monoclonal anti-p-eIF2α (Cat#3398; Cell Signaling; [1:200]), rabbit polyclonal anti-ATF-6 (Cat#24169-1-AP; ProteinTech; [1:50]), BiP (Cat#11587-1-AP; ProteinTech; [1:50]), rabbit monoclonal anti-P-AKT (Cat#4060; Cell Signaling; [1:200]), rabbit monoclonal anti-PTEN (Cat#9188; Cell Signaling; [1:200]), mouse anti-ATF4 (Cat# 10449-1-AP; ProteinTech; [1:200]), rabbit monoclonal anti-Ki67 (Cat# Ab16667; Abcan; [1:250]), goat anti-rabbit IgG AlexaFluor 594 (Cat#A-11037; Invitrogen; [1:500]), goat anti-chicken IgY AlexaFluor 488 (Cat#A11039; Invitrogen; [1:500]), and goat anti-mouse IgG Alexa Fluor 488 (Cat#A11001; Invitrogen; [1:500]). For IHC: AR N-20 (sc-816) rabbit polyclonal [1:200]; Human mitochondrial surface protein, Millipore (Cat# MAB1273, mouse monoclonal [1:200].

Preclinical MRI study

Mice, on average of 6 months old per genotype, were enrolled into a preclinical trial for ISRIB treatment. $Pten^{fl/fl}$ and $Pten^{fl/fl}$;Myc^{Tg} mice had baseline measurements calculated from 0.5 mm slices taken by full-body axial scan with gradient echo sequence on Varian 7T (300 MHz) horizontal bore MRI system. Mice were placed on either Vehicle (HPMT solution, pH: 4) or ISRIB treatment over the course of 6 weeks. Importantly, tumor bearing mice and wildtype littermates (no Pb-cre4 expression) showed no toxicity measured by weight and body conditioning throughout the study (*data not shown*). MRI was initially conducted after 1 wk to examine variations in tumor size from treatment, but tumors remained unaltered, showing minimal growth over baseline. Measurements were then taken after a full 3 wk of treatment where we began to observe changes in tumor size over baseline measurement per mouse. Having observed no toxicity with 2.5 mg/kg of ISRIB treatment daily, the dose was doubled for the remainder of the study before repeating MRI at 6 wk. This study was repeated with a new cohort of mice, taking measurements at the 3 and 6 wk timepoints following the same dosage escalation. Volumes were calculated from DICOM files using OsiriX imaging viewer to integrate drawn outlines on prostate taking from serial images to render 3D measurements. The data from both studies were pulled together, and the mean average fold change to baseline was depicted with standard error of the mean per each arm.

Analysis of immune cell infiltration by flow cytometry

$Pten^{fl/fl}$ and $Pten^{fl/fl}$;Myc^{Tg} mice of tumor bearing age (were placed on either Vehicle (HPMT solution, pH: 4) or ISRIB treatment (5 mg/kg), treated once daily, over the course of 3 weeks. Prostate tissue was microdissected in cold PBS to further remove any non-prostatic tissues, followed by mincing and digested in 2 mg/mL Collagenase II (dissolved in ADMEM/F12). After 1 hr digestion at 37°C with rotation, prostate fragments were washed and centrifuged at 1000 rpm for 5 min at 4°C. Prostate fragments were resuspended in 2 mL of 0.05% Trypsin and digested for another 20 min at 37°C with rotation, with a light vortex every 5 min. Once washed in ADMEM/F12, remaining cells were briefly syringed through 18 and 20-gauge needles followed by straining for single cell collection through 40μm filters prior to brief spin down and resuspension in FACS Buffer (HBSS without calcium, magnesium or phosphorous supplemented with 2% FBS).

For analysis of infiltrating mononuclear cells, isolated cells were blocked with CD16/32 FcB (Cell Culture Facility, UCSF) for 15 min on ice. Samples were then divided into two fractions for staining of either Lymphoid or Myeloid cell markers for 45min on ice in dark. Lymphoid markers were analyzed by staining APC-CD45, PECy7-CD3, PB-CD19, PE-CD4 and PerCPCy5.5-CD8. Myeloid markers were analyzed by staining APC-CD45, PECy7-Ly6G/C, PE-CD11c, PerCPCy5.5-CD14 and Bv510-CD11b. All antibodies were purchased from eBioscience. Samples were then acquired by BD LSR II (Becton Dickinson) and analyzed with FlowJo (FlowJo, LLC). Populations were subdivided into CD4+ (CD45+,CD19-,CD3+,CD4+,CD8-), CD8+ (CD45+,CD19-,CD3+,CD4-,CD8+), Dendtritic (CD45+,CD11c+,CD11b-), Macrophages (CD45+, CD11c-, CD11b+, Ly6G/C-), or Neutrophils (CD45+, CD11c-, CD11b+, Ly6G/C+).

Cell Culture and Reagents

HEK293T cells were obtained from ATCC and maintained in DMEM, 10% FBS, with P/S. Retroviral and lentiviral particles were produced by transfecting cells with the appropriate expression and packaging plasmids using PolyFect Transfection Reagent (Qiagen) and filtering cultured supernatants through a 0.22 μM filter. RWPE-1 prostatic cells were maintained in Keratinocyte Serum Free Medium with 0.05mg/mL of bovine pituitary extract and 5 ng/mL of human recombinant epidermal growth factor (Invitrogen Gibco). shRNA-mediated knock down of PTEN was created by infecting RWPE-1 cells with lentivirus produced in HEK293T cells using pLKO.1 pKate designed vectors targeting PTEN CDS (F.P. 5'-CCGGAGGCGCTATGTGTATTATTATCTCGAGATAATAATAC ACATAGCGCCTTTTTTG-3', R.P. 5'-AATTCAAAAAAGGCGCTATGTGTATTATT ATCTCGAGATAATAATACACATAGCGCCT-3', and 3'UTR (F.P. 5'-CCGGATTTC GGGCACCGCATATTAACTCGAGTTAATATGCGGTGCCCGAAATTTTTTG-3', R.P. 5'-AATTCAAAAAATTTCGGGCACCGCATATTAACTCGAGTTAATATGCGG TGCCCGAAAT-3'). Cells were sorted for pKate expression and plated to single cell to create isogenic cell lines. Isogenic RWPE-1 cells were then infected by retroviral supernatant with human c-Myc-GFP or GFP expression vectors followed by appropriate selection with blasticidin (5 μg/mL).

Apoptosis analysis by flow cytometry

Cells were strained to single cell suspensions in BD binding buffer then stained for APC-Annexin V (Cat#BDB550475; BD Pharmingen; [1:100]) for 20 min RT in dark. Propidium iodide (Sigma) was added to samples within 5 min prior to data collection, followed by brief vortex. Samples were acquired using BD Verse (Becton Dickinson) and analyzed with FlowJo. At least 20,000 events were recorded per sample condition and Annexin V+ (APC+) populations were quantified. Data was pulled from three or more biological replicates. For ISRIB experiments, cells were pretreated with 500 nM of ISRIB for 9 hours prior to collection.

Cell Proliferation

RWPE-1 human cell lines were counted and plated to a 96-well plate in quadruplet per condition tested. After 36hr, cells reached approximately 70% confluency and were treated with DMSO, 500nM ISRIB, or media containing 1% Bleach as a negative control in 90 uL/well. After 8 hr, 10 uL of the CCK-8 solution was added to each well followed by 1 hr of final incubation following manufacturer's instructions (cell counting kit-8, Enzo: ALX-850-039). Absorbance was read at 450nm using a BioTeK microplate reader. The experiment was repeated, quantified relative to Ctrl cells treated with DMSO per experiment, and averages pulled for analysis.

Development of PDX lines

Tumor tissues were harvested and evaluated by pathologists after retrieval of the specimen from the operating room. The tumor pieces were then immediately placed in 10 mL of RPMI 1650 medium and cut into ~3–5 mm per cubed side for implantation. Tumor bits were implanted subcutaneously in 6–8 weeks old intact male NSG mice (UCSF Breeding Core). Mice were monitored post implantation for initial growth weekly. Tumors that grew were passed into new intact male NSG mice. After three passages, they were set as an indication of an established PDX line and cryopreserved. We retained tumor sections and

cryopreserved frozen tissue after each passage, and compared histological characteristic and growth curve to original tumor to ensure that the subsequent passages maintained the integrity of tumor characteristic. For this, subcutaneous PDX tumors were formalin fixed and paraffin embedded followed by 5 μm sections to compare histopathology to originating tissue with hematoxylin and eosin (H&E). From 8 patient tumors, 2 PDX lines were successfully developed. Tumor samples were harvested from later passages (>3) and frozen or embedded in paraffin for characterization. The metastatic and primary tumor harboring PDX lines were maintained by constant passaging in male NSG mice. The castrated resistance prostate cancer (CRPC) PDX model was generated by implanting CRPC tissues into the renal capsule. Tumor was derived from a patient with metastatic prostate cancer despite prolonged treatment with complete androgen blockage using Lupron (androgen deprivation therapy) and 2nd generation antiandrogen (from UCD collaboration). Three weeks after implantation of the human tumor under the mouse renal capsule, we have observed tumor disseminate and metastasize to the liver, kidney, abdominal lymph nodes and spleen. Histological analysis was used to compare each passage to the original tumor and distal sites of metastasis to ensure preservation of the integrity of the model. Animals were maintained for studies until clinical signs of morbidity were observed including: 15-20% weight loss, hunched posture, low activity, BSC $\leq$ 2, or paralysis of one or more limbs due to the metastatic invasion. Once any of the above were observed, animals were promptly imaged (within 36 hours) and then euthanized in accordance with our protocols.

Preclinical PDX study

Pharmacologic approach: studies were conducted with male NSG mice (6-8 weeks old) engrafted subcutaneously into the right hind flank with metastatic and primary PDX tumors. Once the tumors reached 4 mm in diameter, 8 mice/group were randomized to receive vehicle (control) or 10 mg/kg ISRIB, daily by oral gavage (treatment). Tumor volume and weight were recorded every three days to evaluate changes in tumor volume and toxicity; no toxicity was observed at 10 mg/kg daily dose over the course of the study. The volume of the tumor was measured twice a week until the volume reached 2 cm in diameter, and then mice were euthanized according to our institutional protocol for tumor reaching ethical limits. For the mCRPC PDX preclinical studies with ISRIB, the male NSG mice bearing the patient derived mCRPC tumor previously established were subjected to prostate-specific membrane antigen (PSMA) ^{68}Ga-PSMA PET/CT imaging at 21 days from mCRPC tumor tissue (0.5 -1 mm) renal capsule engraftment. Mice with liver metastasis found on PSMA PET/CT were randomized into vehicle (n = 5) or ISRIB (n = 5) treatment cohorts. Mice that did not tolerate PSMA scan or oral gavage the day after randomization were excluded; final analysis consisted of n = 3 mice for control and n = 3 for ISRIB treatment group. After randomization, mice were orally gavage with vehicle (control) or 10 mg/kg ISRIB daily for up to two weeks, a predetermine timepoint. Subsequent PSMA PET/CT scan were carried out at one week after treatment to monitor metastasis progression or response to ISRIB treatment. Mice were euthanized if we observed two or more metastatic lesions on PSMA PET/CT post treatment day 7, in accordance to our institution protocol. All surviving mice were euthanized at the end of the two-week study according to predetermined endpoint. Tissues was harvested for histochemistry analysis to confirm radiographical finding at time of euthanasia.

Genetic approach: Intratumor delivery of small interfering RNA targeting ATF4 (Activating Factor 4) in PDX mice bearing mPCa tumor (lymph node metastasis) were used to evaluate the specific effect of ATF4 gene knockdown on tumor cell apoptosis and proliferation. Briefly, NSG mice with mPCa tumors (n = 5 per group) were randomized to be treated with Accell Green Non-targeting siRNA (Dharmacon, Cat. #D-001950) or Accell Human ATF4 siRNA (Dharmacon, Cat. #E-005125). We used green fluorescence labeled siRNA to observe the specific area of delivery to study siRNA effect of ATF4 knockdown on apoptosis and proliferation of tumor cells. Treatment by intratumor injection of 5 µg jetPEI/Non-targeting siRNA to the left flank tumor and 5 µg of jetPEI/ATF4-siRNA to the right flank tumor within the same mouse to decrease variables in the treated and untreated group. After seven days of intratumor delivery of siRNA to ATF4, tumor was harvested and subject to immuno-histological analysis.

^{68}Ga-PSMA PET preclinical imaging

Imaging was conducted at the UCSF MicroPET/CT, Optical Imaging Core Facility using an Inveon small-animal PET/CT scanner (Siemens) at two distinct time points; Day 0 marking start of treatment and Day 7 post one week of treatment treatment. The mice were injected with approximately 300µCi of ^{68}Ga-PSMA via the tail vein. One hour after injection, they were anesthetized with 2% isoflurane and imaged for 10–20 min to acquire approximately 20 million coincident events. Data were analyzed using AMIDE software.

TUNEL assay for apoptosis

Formalin-fixed paraffin embedded tissues from mPCa and pPCa bearing PDXs treated with 10 mg/kg ISRIB or vehicle for up to 2 weeks were sectioned and mounted on slides by core facility. Tissue slides were de-waxed, rehydrated, and then incubated with 20 ug/mL Proteinase K (Roche) in 10mM Tris-HCl for 15 minutes at 25°C. Apoptotic cells were detected by the presence of DNA strand breaks as marked by Terminal deoxynucleotidyl transferase dUTP nick end labeling using the in-Situ Cell Death Detection Kit, TMR red (Roche) according to the manufacturer's protocol. Sections were counterstained with DAPI, mounted, and imaged. TUNEL staining was evaluated by manually counting TUNEL positive nuclei and total nuclei present in randomly taken pictures of at least four high power fields (40X) representing three separate tumors per condition.

***In vivo* protein synthesis**

After tumors reached 4mm in diameter, after implantation, the PDX cohorts were randomized to receive treatment with vehicle or ISRIB (Sigma) (p.o. 5mg/kg for 5 days). OP-Puromycin (Puro) (Medchem Source LLP) was reconstituted in PBS with adjusted pH of 6.5 and stored in aliquots at -20 °C. PDX models were injected with 50 mg/kg by intraperitoneal injection (IP) and a control mouse was injected with PBS only as a sham to subtract background expression during analysis. One hour after injection, each mouse was quickly euthanized and tumors dissected, minced, and digested for creating single cell dissociation. Briefly, minced tissue is digested for 1-2hr in collegenase followed by 20 min in 0.05% trypsin, manually dissociated by needle and syringe, and then strain to single cell for counting by hemocytometer. Tumor cells were then labeled with CD235, CD31 and CD41, all of which conjugated to e450 as a negative gate, and wrapped in foil for 20 min shaking at 4 °C. Cells were then fixed in 0.5 mL PFA in PBS for 15 min on ice, washed in

cold PBS, and permeabilized in the dark using PBS with 3% FBS and 0.1% Saponin. Click-iT reaction (Invitrogen) was performed following manual with cycloaddition conjugation to Alexa555 with 30 min interaction at room temperature with light protection. Data was acquired using a BD LSRII and analyzed with FlowJo to calculate the fluorescence intensity of each sample and analyzed with FlowJo to calculate the fluorescence intensity of each sample. For quantification, the relative rates of protein synthesis depicted by OP-Puro signals were calculated by subtracting the auto-fluorescence background from sham (PBS injected) mice from each sample by Mean Fluorescence Intensity (MFI). Normalized MFI per each arm was plotted with standard deviation of the mean.

Patient population and Tissue microarray construction

Prostate tissue samples were taken from a series of 424 men who underwent radical prostatectomy without neoadjuvant or adjuvant therapy between at University of California, San Francisco with follow up of 10 years. Clinical data including patient age at surgery, race, BMI, clinical stage, Gleason score, preoperative PSA, surgical specimen pathology (tumor grade, surgical margin status, seminal vesicles invasion, extracapsular extension, and lymph node metastasis), postoperative PSA, and biochemical recurrence, salvage radiation, visceral and bone metastasis and prostate cancer specific mortality status was queried from the University of California, San Francisco Urologic Oncology Data Base (UCSF UODB). The median follow up was 10 years, mean age of diagnosis was 58 year old, mean PSA at diagnosis was 7. Importantly, this study adhered to the principles of the prospective specimen and clinical data collection under a standardized protocol to minimize variables that could affect the expression of phospho-protein including time of banking after tissue devasculization. The prospective clinical data collection in UCSF UODB minimized potential selection bias.

Tumor tissue and benign stromal tissue were reviewed and selected by expert pathologists (J.S.). The tissue microarray (TMA) was constructed using a Manual Tissue Arrayer (MTA, Beecher Instruments Inc.). Tumor was cored from formalin fixed paraffin embedded surgical tissue block using 0.6mm diameter coring needles, taken from representative area of significant tumor. The resulting TMA was the largest one created at UCSF consisted of a total of 424 tumor and 300 stromal benign tissue. The TMA was sectioned into 4-micron slices and stained as described under Immunofluorescence microscopy. Specimen processing, staining and quantification were performed blinded to the TMA location and clinical data. The following antibodies were used: chicken polyclonal anti-CK8 (Cat#ab107115), Abcam; PTEN (Cat#9188), Cell signaling; Peif2a (Cat#3398), Cell signaling; cMyc (Cat#ab32), Abcam. All concentration used was according to the company's manual. The signals were quantified by Zeiss analysis program.

Statistical Analysis

All data are presented as the average mean of values with error bars representing the standard deviation of the mean with at least three independent biological or technical replicates experiments. Unless otherwise noted, p-values generally indicate statistical significance in an unpaired, two-tailed t-test denoted by * = $P<0.05$, ** = $P<0.01$, *** = $P<0.001$.

For TMA analysis, exposure variables of interest were gene expression values for PTEN, c-Myc, and P-eIF2α (phosphorylation of eIF2α). PTEN loss were defined as having an expression level measured by relative mean fluorescence intensity lower (negative value) than adjacent benign tissue. High c-Myc expression was defined as having higher than or equal to 25% mean fluorescence intensity over the adjacent benign stromal tissue. High P-eIF2α expression was defined as having higher than or equal to 25% mean fluorescence intensity over the adjacent benign stromal tissue (≥ the 25th percentile value). Three composite exposure variables also were created: 3-level PTEN loss with high P-eIF2α versus PTEN loss with low P-eIF2α versus no loss of PTEN. Independent covariates included characteristics at diagnosis age (years), PSA (ng/mL), race, biopsy Gleason grade, clinical T-stage and surgical pathology at RP (Gleason grade, pathologic T-stage and N-stage, surgical margins). Outcome events were defined as any clinical relapse/progression, defined as either metastasis detected on imagining (bone scan, MRI, CT) after RP or prostate cancer specific mortality (PCSM). Independent variables were described with means, medians and ANOVA if continuous values and frequency tables, chi-square and Wilcoxon if categorical values. Pearson and Spearman coefficients were used to determine inter-item correlations between independent variables. Logistic regression was used to evaluate associations between exposure variables and adverse pathology at RP, adjusted for age, PSA, biopsy Gleason score, and clinical T-stage. Lifetable estimates, Kaplan-Meier curves, log-rank test, and Cox proportional hazards regression were used to test for associations between exposure variables and time-to-event outcomes. Factors that could influence the outcome were adjusted in the Cox model, including patient's clinical and pathological features that could affect the outcome, including patient's age, PSA, pathologic cancer grade (Gleason score 6 vs 7 or higher) and pathological staging (T2 vs T3 or higher) at time of surgery. A p-value <0.05 was considered significant. All analysis was completed with SAS 9.4 for Windows. We reported Harrell's C index, the concordance statistic generated for right-censored data from the Cox proportional hazards regression procedure using SAS 9.4 for Windows.

SUPPLEMENTARY FIGURE LEGENDS

Supplementary Figure 1. Myc^{TG} and Pten loss synergize for aggressive PCa development. (**A**) Schematic of prostate specific loss of PTEN or MYC overexpression from transgene construct depicted on right highlighting the promoter, Lox-STOP-Lox site, HA-c-Myc, and IRES upstream of the palmitoylated-eGFP. (**B**) Representative images from H&E or IF staining of prostate markers Ck5 and Ck8 in relation to transgenic GFP expression within 10 wk old anterior prostate tissue. (**C**) Representative H&E images for MycTg anterior prostate tissue at indicated age. (**D**) Representative IF images of MYC/Ck5 co-staining with Dapi on 10 wk old anterior prostate tissue, *left panel.* Cells with MYC expression were counted relative to total number of cells as a percentage, and the relative fold change to wildtype was plotted (*right panel*, n = 3 mice per arm, with four images averaged per mouse, ±SEM). (**E**) Representative IF images of Phospho-Histone3 (PHis3)/Ck5 co-staining with Dapi on 10 wk old anterior prostate tissue, *left panel*. Cells with nuclear PHis3 expression were counted relative to total number of cells as a percentage, and relative fold change to wildtype tissue was plotted (*right panel*, n = 3 mice

per arm, with at least three images averaged per mouse, ±SEM). **P < 0.01, *P < 0.05, n.s. represents non-significantly different P >0.05, two-tailed, t-test.

Supplementary Figure 2. Unfolded protein response is activated in PCa. (**A**) Representative IF images of ATF6 or P-IRE1/Ck5 co-staining with Dapi on 10 wk old anterior prostate tissue, *left panel*. Cells with nuclear ATF6f expression representing the transcriptional activator domain (white arrows) were counted relative to total number of cells as a percentage, and the relative fold change to wildtype was plotted. P-IRE1 expression relative to Dapi was quantified as fold (n = 3 mice per arm, with four images averaged per mouse, ±SEM). (**B**) Representative IF images of BiP/Ck5 co-staining with Dapi on 10 wk old anterior prostate tissue, *left panel*. BiP expression was counted relative to total number of cells as a percentage, and the relative fold change to wildtype was plotted (n = 3 mice per arm, with at least three images averaged per mouse, ±SEM). (**C**) Representative IF image of GFP from the Myc transgene expression co-stained with P-eIF2α and Dapi in anterior prostate tissue with neoplasia. **P < 0.01, *P < 0.05, n.s. represents non-significantly different P >0.05, two-tailed, t-test.

Supplementary Figure 3. PERK loss blocks PCa progression and decreases P-eIF2α expression. (**A**) A model to depict that normal stress response downstream of PERK activation to phosphorylate eIF2α during stress, which inhibits GEF activity of eIF2B. With ISRIB treatment, the eIF2B decamer stabilizes and increases affinity for eIF2α for normal GEF activity. (**B**) A model depicting the cross of a probasin Cre specific loss of PERK into the GEMMs. (**C**) Total dehydrated prostate weights from 10 wk old mice were averaged per genotype (n = 3-4 mice per arm, ±SEM). (**D**) Representative H&E images from 10 wk old mice showing anterior prostate gland. (**E**) Quantification of nuclear P-His3 expression on 10 wk old anterior prostate tissue counted relative to total number of cells as a percentage, with relative fold change to wildtype tissue plotted (from fig. S1E, n = 3-4 mice per arm, with at least three images averaged per mouse, ±SEM). (**F**) Representative IF images of P-eIF2α/Ck5 co-staining with Dapi on 10 wk old anterior prostate tissue, *left panel*, and directly within areas of PIN, *middle panel.* P-eIF2α expression was counted relative to total number of cells, and the relative fold change to wildtype was plotted (from Fig. 2A, n = 3-4 mice per arm, with four images averaged per mouse, ±SEM). **P < 0.01, *P < 0.05, n.s. represents non-significantly different P >0.05, two-tailed, t-test.

Supplementary Figure 4. Loss of P-eIF2a activity by ISRIB does not substantially alter immune infiltrating cells. (**A**) Percentage of CD45+ immune infiltrating cells in the labeled prostatic tissue after three weeks of either vehicle or ISRIB treatment daily (n = 3-5 mice per arm, ±SEM). (**B**) Percentage of CD45+ cells that depicted dendritic, macrophage, or neutrophil lineage markers. (**C**) Percentage of CD45+, CD3+, CD109- cells that depicted CD4+ or CD8+ T-cell markers. n.s. represents P >0.05, t-test.

Supplementary Figure 5. Effects of pharmacological inhibition of P-eIF2α activity in human cell lines growth by ISRIB. (**A**) Relative proliferation in RWPE-1 cell lines quantified by cell counting kit-8 (cck8). Cells were treated with DMSO, 500nM of ISRIB, or media containing 1% Bleach as a negative control (Neg crtl) for 9hr. (n = 3, ±SD) **P < 0.01, two-tailed, t-test.

Supplementary Figure 6. Tissue microarray of prospectively collected specimen from 424 men with clinically significant PCa undergoing curative treatment. (**A**) Representative IF of P-eIF2α on tumor and adjacent benign tissue from microarray (TMA) consisting of 424 tumors and 300 benign tissue randomly selected from men who underwent radical prostatectomy at UCSF, *left panel*. Representative quantification of one tissue sample mean IF intensity, normalized to adjacent benign tissue for expression levels of P-eIF2α was done blinded to the clinical and pathological outcome and tumor location on the TMA, *right panel*. For each section, three images were averaged, ***P < 0.001, t-test. (**B**) Representative IF images of PTEN loss and PTEN normal tumors, and high MYC and low MYC expression from the TMA. (**C**) Kaplan-Meier analysis of clinical progression (defined as visceral or bone metastasis or prostate cancer specific mortality (PCSM)) free survival for patients with low MYC level versus high MYC level relative to P-eIF2α expression.

Supplementary Figure 7. Marked increase in apoptosis in metastatic tumor after treatment with ISRIB or siRNA for ATF4. (**A**) Representative IF images of PTEN co-staining with Dapi from adjacent benign tissue, primary tumor, or metastatic lymph node tumor from the PDX. (**B**) Representative western blot analysis of cleaved caspase 3 in primary (pPCa) and metastasis (mPCa) bearing PDX tumors treated with 10 mg/kg ISRIB or vehicle for two weeks. (**D**) Model depicting siRNA delivery to mPCa tumors, *upper panel*. Representative IF for tumors treated with siRNA for scramble (scrm) or ATF4 showing expression of ATF 4 (left), TUNEL (middle) and Ki67 (right), *middle panel*. *Bottom panel*, quantification of ATF4 expression within tumor treated in intratumor delivery of siRNA using mean fluorescence intensity. Quantification for TUNEL and Ki67 were completed as percentage of cells positive compared to Dapi. n = 3, **P < 0.01, t-test.

Supplementary Figure 8. Generation of a patient derived xenograft (PDX) to best recapitulate metastatic dissemination and castration-resistant PCa (mCRPC). (**A**) Representative H&E staining of distant metastatic lesions taken from primary site of implantation (mCRPC tumor), left kidney, lymph node, liver and spleen at 6 weeks after implantation of the original tumor taken from a patient with mCRPC. Immunohistochemistry analysis of androgen receptor and human mitochondria were used to confirm the presence of prostate cancer tissue of human origin in the mouse organs. (**B**) Representative immunofluorescent images P-eIF2α (cytosolic), androgen receptor (nuclear localization), MYC (nuclear localization) and PTEN in the tumor area co-staining with Dapi from adjacent benign mouse tissue and metastatic tumor from the mCRPC PDX. (**C**) Representative of ^{18}F-DG PET/CT and ^{68}Ga-PSMA-11 PET/CT scan on the same mouse bearing mCRPC tumor, performed one day apart showing metastatic liver lesion only visible using more sensitive ^{68}Ga-PSMA-11 agent. (**D**) Western blot expression of androgen receptor (AR), P-eIF2α, total eIF2α, and actin in four different lines of PDX with various stages of cancer pPCa (taken from primary prostate specimen) mPCa (taken from lymph node metastasis in a patient with hormone sensitive metastatic disease) and mCRPC (taken from metastatic castration resistant tumor). Line 1 and 2 are taken from same patient while line 3, 4 are from different individual patient.

Table 1. Characteristics of tissue microarray specimen from 424 men with clinically significant PCa. Baseline characteristic of the TMA cohort with the average age of diagnosis of 58-year-old. 57% of the cohort had pathological grade 7 or higher and 75% of the men had organ confined disease (pathological stage T2). Median follow up was 10 yrs.

REFERENCES

1 Matsuda, T. & Cepko, C. L. Electroporation and RNA interference in the rodent retina in vivo and in vitro. *Proc Natl Acad Sci U S A* **101**, 16-22, doi:10.1073/pnas.2235688100 (2004).

2 Miyazaki, J. *et al.* Expression vector system based on the chicken beta-actin promoter directs efficient production of interleukin-5. *Gene* **79**, 269-277 (1989).

3 Jackson, E. L. *et al.* Analysis of lung tumor initiation and progression using conditional expression of oncogenic K-ras. *Gene Dev* **15**, 3243-3248, doi:DOI 10.1101/gad.943001 (2001).

4 Rees, S. *et al.* Bicistronic vector for the creation of stable mammalian cell lines that predisposes all antibiotic-resistant cells to express recombinant protein. *Biotechniques* **20**, 102-& (1996).

5 Okada, A., Lansford, R., Weimann, J. M., Fraser, S. E. & McConnell, S. E. Imaging cells in the developing nervous system with retrovirus expressing modified green fluorescent protein. *Experimental Neurology* **156**, 394-406, doi:DOI 10.1006/exnr.1999.7033 (1999).

6 Lesche, R. *et al.* Cre/loxP-mediated inactivation of the murine Pten tumor suppressor gene. *Genesis* **32**, 148-149 (2002).

7 Drost, J. *et al.* Organoid culture systems for prostate epithelial and cancer tissue. *Nature Protocols* **11**, 347-358, doi:10.1038/nprot.2016.006 (2016).

Supplementary Figure 1

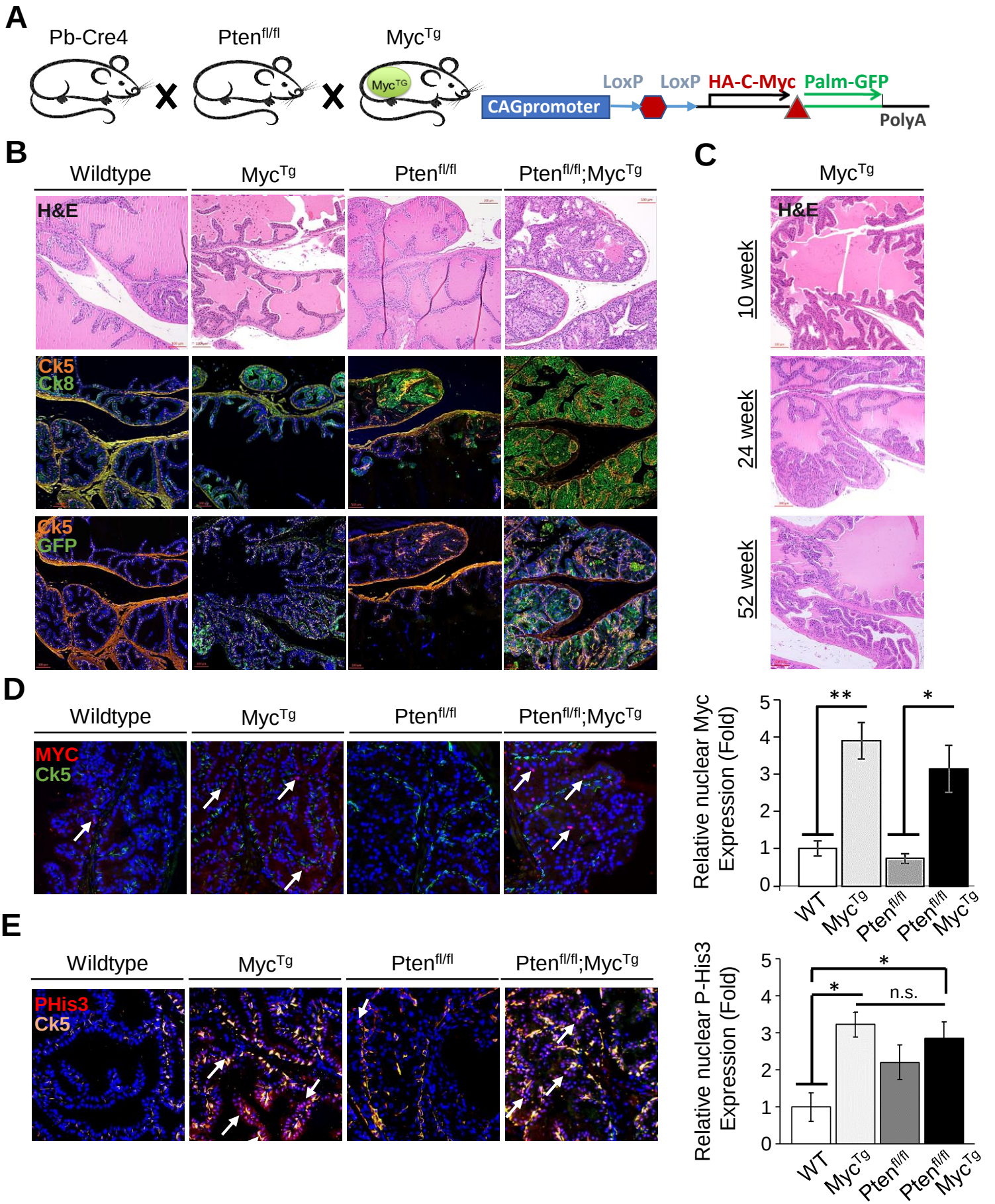

Supplementary Figure 2

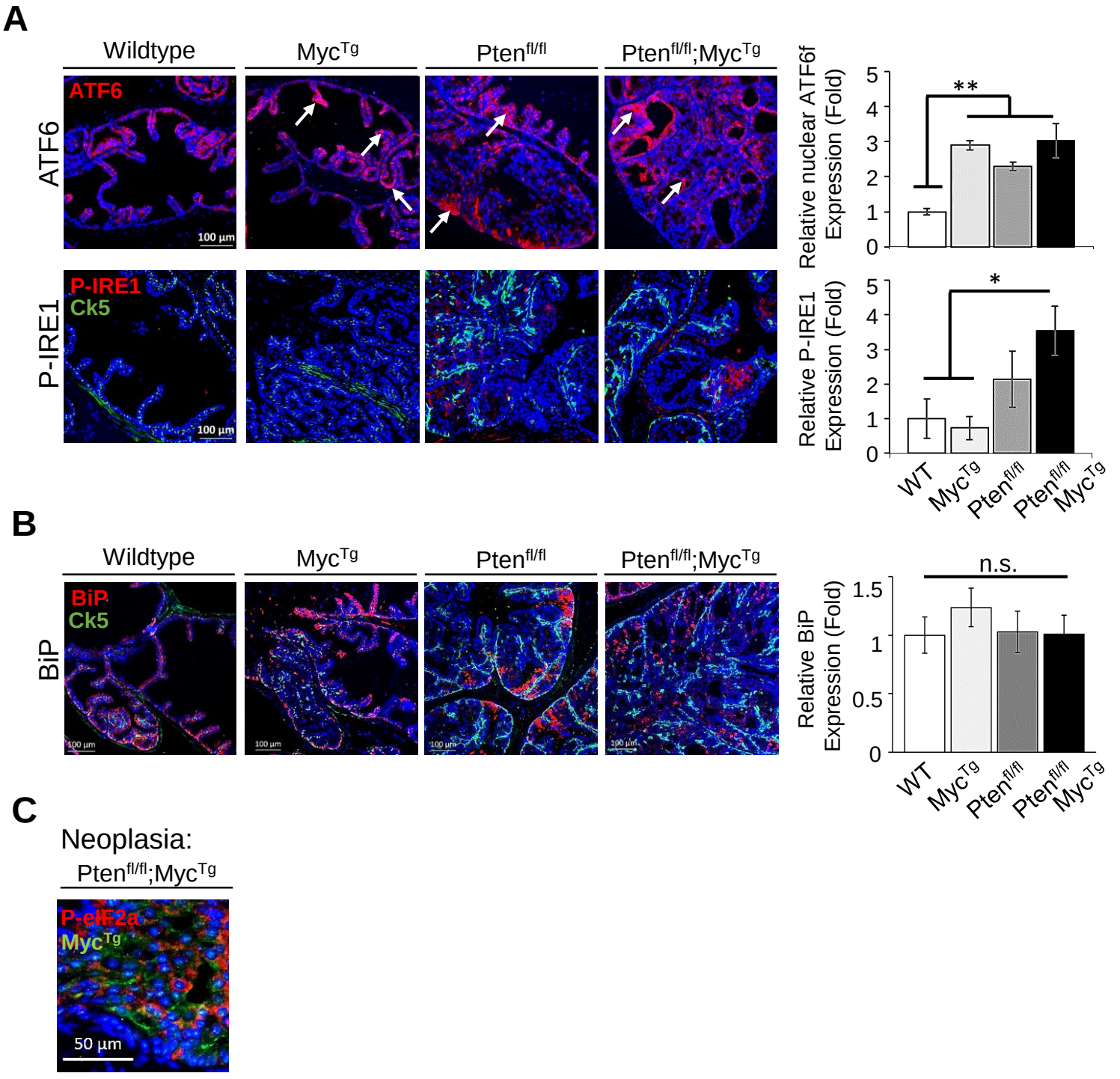

Supplementary Figure 3

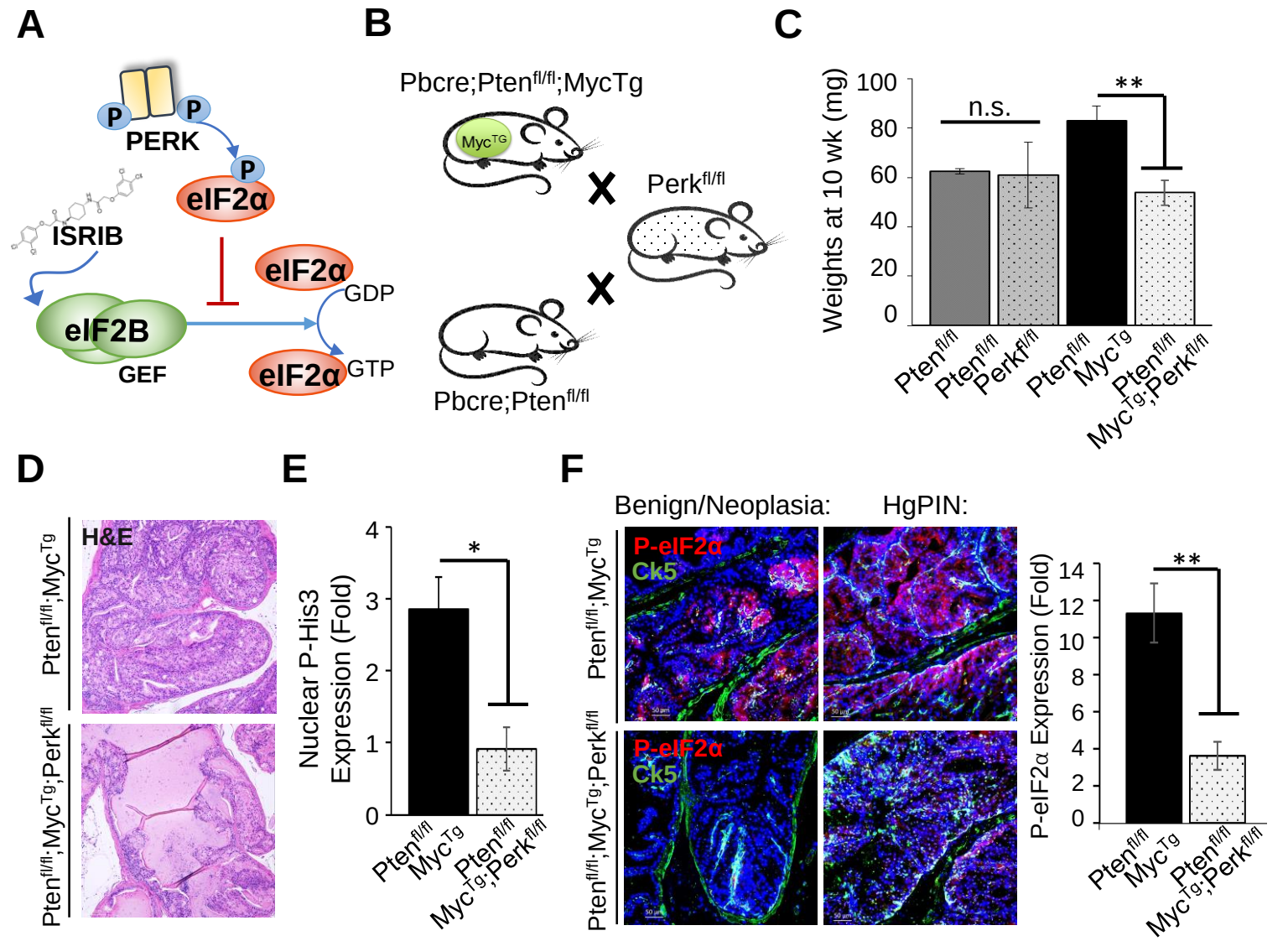

Supplementary Figure 4

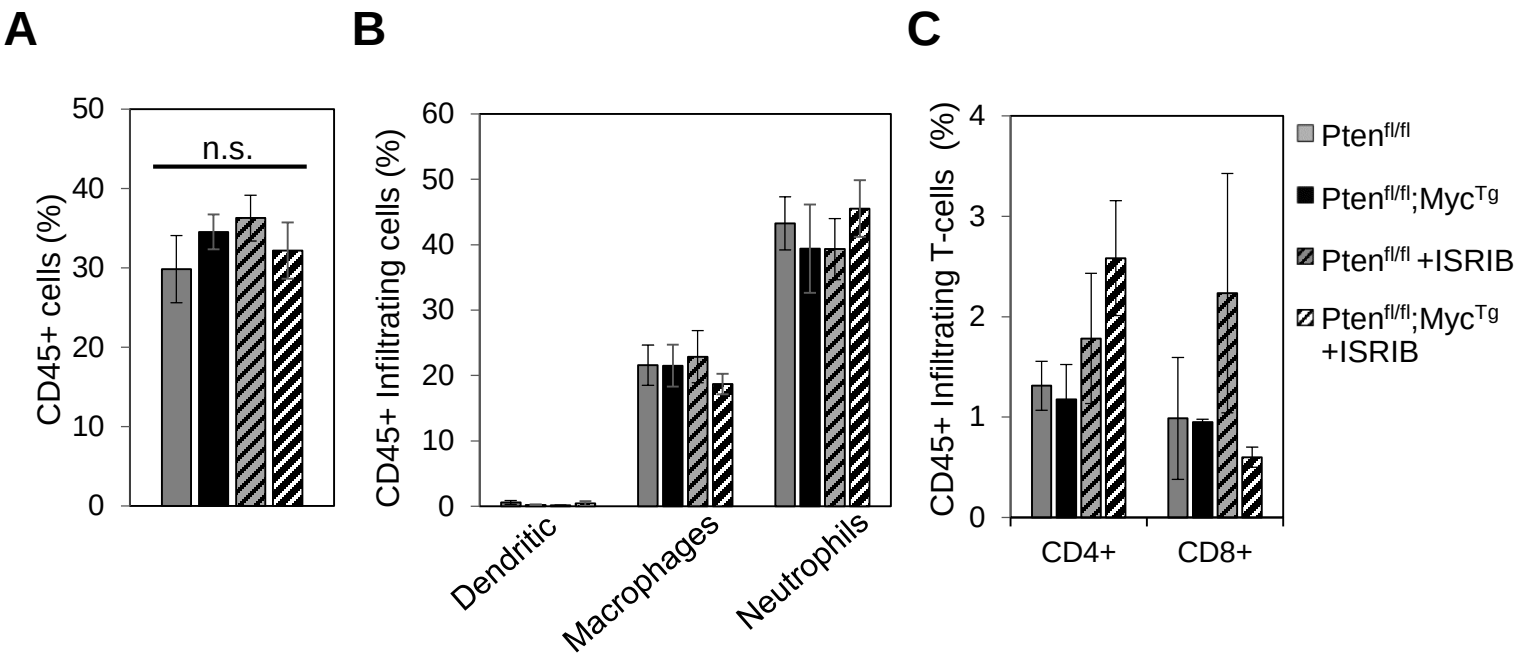

Supplementary Figure 5

A

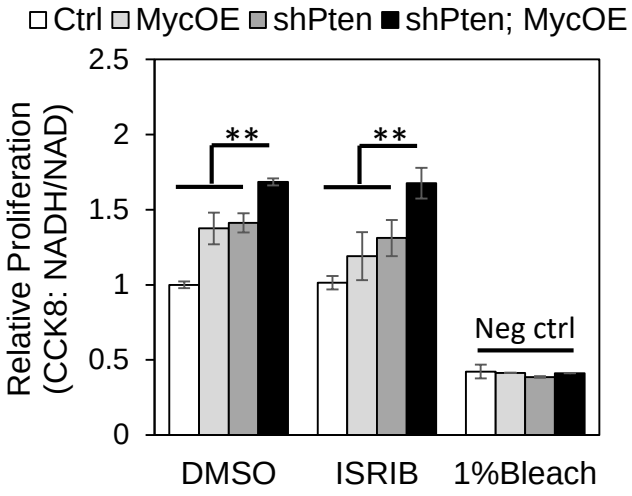

Table 1

Patient characteristics:

Patient characteristics	Value	N	(%)
Race/ethnicity	Native American	1	0
	Asian/Pacific Islander	13	3
	African American	14	3
	Caucasian	359	85
	Mixed	25	6
	Unknown	12	3
Biopsy Gleason grade	3+3	263	64
	3+4	95	23
	4+3	25	6
	8-10	29	7
	Missing	12	.
Clinical T-stage	T2	296	98
	T3	5	2
	T4	2	1
	Missing	121	.
Path Gleason grade	3+3	184	43
	3+4	173	41
	4+3	45	11
	8-10	22	5
Pathologic T-stage	T2	313	75
	T3	102	24
	T4	5	1
	Missing	4	.
Pathologic N-stage	NX	200	48
	N0	208	50
	N1	7	2
	Missing	9	.
Surgical margins	No	354	83
	Yes	70	17
Adverse path (GS≥4+3 or pT3a/pN1)	No	291	69
	Yes	133	31

Supplementary Figure 6

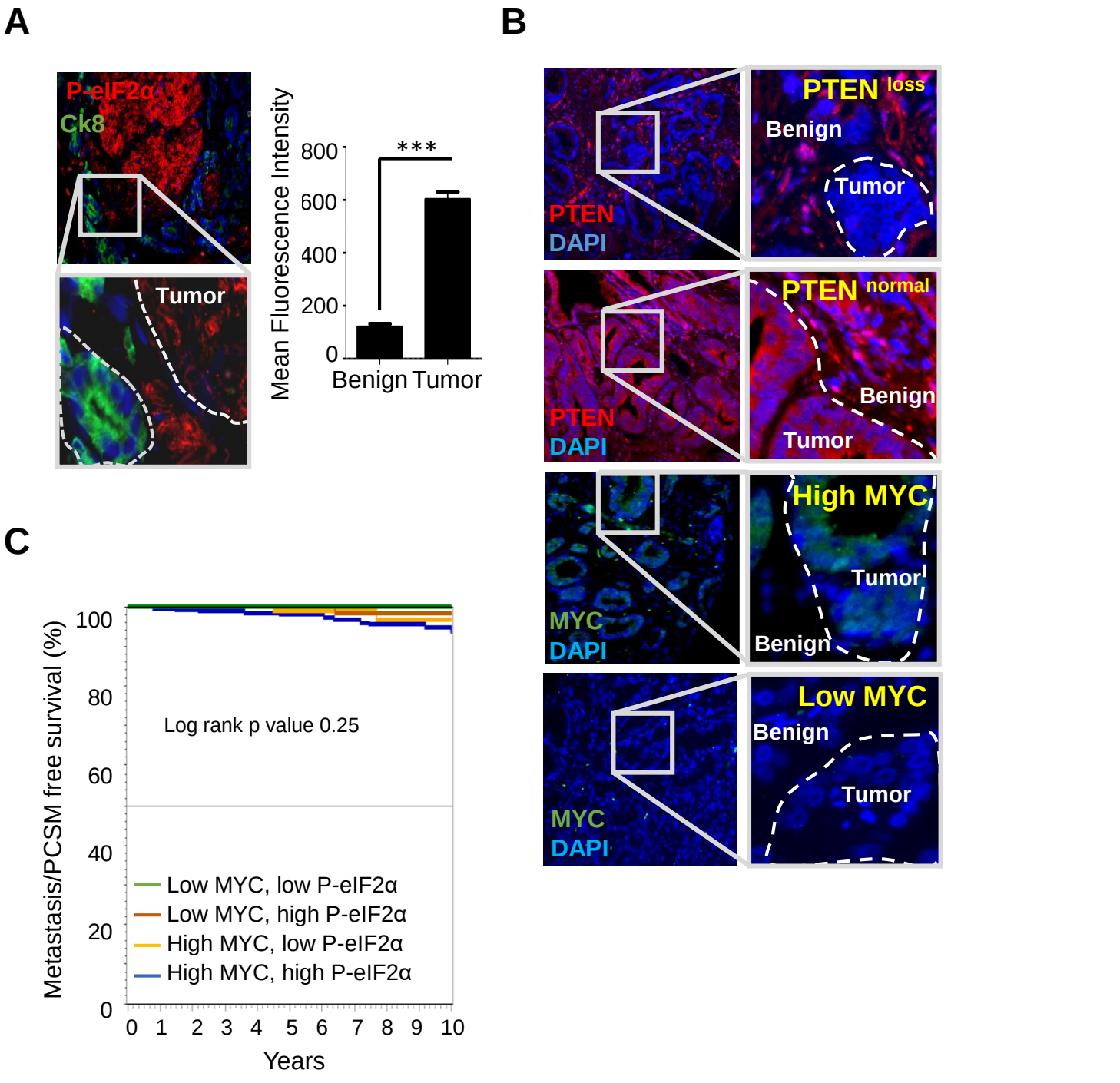

Supplementary Figure 7

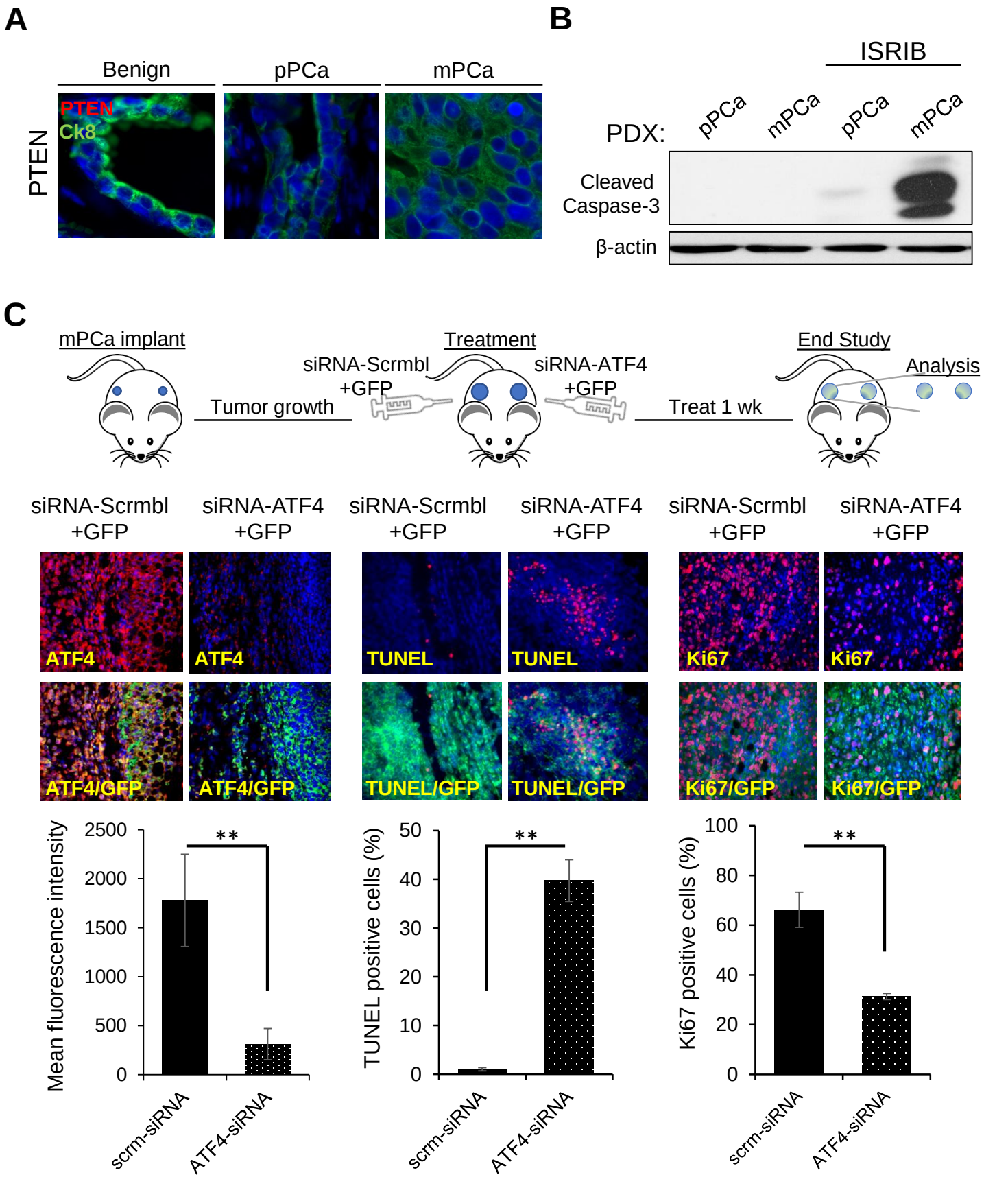

Supplementary Figure 8